7th International Conference on Debris-Flow Hazards Mitigation

# Experimental examination for influence of debris-flow hydrograph on development processes of debris-flow fan

Haruka Tsunetaka[a,]*, Norifumi Hotta[b], Yuichi Sakai[b], Yuki Nishiguchi[c], Junya Hina[c]

[a]*Forestry and Forest Products Research Institute, Matsunosato 1,Tsukuba 305-8687, Japan*
[b] *Gradual School of Agricaultural and Life Sciences, The University of Tokyo, Bunkyo-ku Yayoi -1-1-1, Tokyo 113-8657, Japan*
[c]*Construction Thecnology Institute Co., Ltd., Onigakubo 1047-27, Tsukuba 300-2651, Japan*

**Abstract**

In order to assess the influence of different flow hydrographs on fan development processes, we carried out flume tests using a sloped channel (15°, 10 cm wide) with a deposition area (slope decreases from 12° to 3° at a rate of 3° per m). The channel was filled with 0.12 $m^3$ of sediment materials. Debris flows were generated by the entrainment of filled sediment via a steady water flow (0.003 $m^3/s$). We used two types of water supply systems: single surge (60 second duration) and double surge (first surge lasting 50 seconds followed by a second surge with 45 second duration). For the double surge system, there was a 60 second pause in water supply between two surges. Fan formation processes in the deposition area were captured on video, and synchronized interval photography (1 second intervals) using three digital cameras. Time-series changes in fan topography were detected using Structure from Motion photogrammetry (SfM), while flow directions were detected using Particle Image Velocimetry (PIV). The results demonstrate that the flows of single surge cases produced asymmetric fans that inclined to one side due to an increase in the runout distance of the continuing flow. In contrast, the first surge of the double surge cases produced fans that were relatively symmetric. Despite this, the second surge continuously changed flow direction while stopping in the deposition area, and covered the symmetric surge produced by the first surge. Consequently, the final topography of double surge cases was highly variable, despite having the same water supply conditions.

*Keywords:* Debris-flow fan; Flume test; SfM-MVS; PIV

## 1. Introduction

Debris-flow deposition plays a critical role in debris-flow fan development (De Haas et al., 2018) and has been linked to many debris-flow disasters (Dowling and Santi, 2014). The ability to estimate and predict debris-flow deposition in the vicinity of the outlet of the feeder channel is important to prevent debris-flow disasters and to interpret the long-term sedimentation regime on alluvial fans. Numerical simulations based on the governing equation of debris flow can be an effective means to estimate the magnitude and extent of deposition. A comparison between the results from simulations and flume tests has demonstrated that simulations can account for almost all of the deposition range of debris-flow fan (e.g., Nakagawa and Takahashi, 1997).

Almost all of these simulations have focused on the occurrence of single debris-flow. However, recent field observations (Pederson et al., 2016), flume tests (De Haas et al., 2016), and numerical simulations (Chen et al., 2017) revealed debris-flow surges on alluvial fans are altered by existing topography. Therefore, in the case where multiple surges had intermittently descended, there is the possibility that the varying fan topography would be produced because of topographic differences resulting from the deposition of the previous surges.

However, direct field measurement of debris-flow rate and fan formation processes are difficult due to the low frequency of debris flows and their destructive power. Accordingly, the influence of debris-flow hydrograph in accordance with the number of surges on fan formation processes has not been fully understood. In this study, we examine the changes in topography and flow directions on the fan with differences in the debris-flow hydrograph, based on the comparison of fan formation processes between single or double debris-flow surges.

* Corresponding author e-mail address*: tsunetakaharuka@ffpri.affrc.go.jp*

## 2. Methods

We identified differences in the debris-flow fans among cases based on flume test results, using Structure from Motion - Multi View Stereo (SfM-MVS) and Particle Image Velocimetry (PIV).

### *2.1. Flume test setting*

The flume channel used for the experiments was 8 m long and 10 cm wide with a 15° slope. The dimensions are approximately one-hundredth of real-life debris-flow torrents in scale (Fig. 1). The deposition area was located at the end of the channel (Fig. 1a), and the slope decreases from 12° to 3° at a rate of 3° per meter (Fig. 1b). Square grid lines (20 cm × 20 cm) were drawn in the deposition area in order to measure the runout distance and inundation range (Fig. 1a).

The section in the lower end of the channel (7 m long) was filled with 0.12 $m^3$ of sediment particles (Fig. 1b). The deposition depth was set between 0 to 0.2 m to being smoothly connected at the upper and lower end of deposits. Consequently, the slope of the initial bed changed at the lower end of deposits from 15° (in the channel) to 12° slope (in the deposition area). The filled sediment consisted of multi-granular particles (2.14 to 7 mm in size), and the $D_{50}$ was approximately 3.7 mm. We generated debris flows through entrainment of the filled sediment using steady water flow supplied from the top of the channel. The flow rate was set at 0.003 $m^3$/s.

Two types of water supply systems, single surge and double surge, were employed to compare the influence of debris-flow hydrograph. There is a time lag between the start of overflow and the valve closing because the water supply was controlled by the opening and closing of a valve. For the single surge system, the water was supplied 60 seconds after the start of overflow from the top of the channel. Consequently, a single debris-flow surge was generated. For the double surge system, the water was supplied 50 seconds after the overflow, and again after a 60 second pause in water supply, the valve was opened for 45 seconds. As a result, the two surges descended with an interval of approximately 65 seconds.

### *2.2. Measurement contents and SfM-MVS, PIV*

Four digital single-lens reflex cameras (DSLRs) were installed approximately 2.5 m above the point where the bed slope changed from 9° to 6° to capture the development of the debris-flow fans through photographs and video footage (Fig. 1b). Three of the DSLRs (D5100, Nikon Co.) were automatically synchronized using the remote shutter. The photographs were captured with 1-second intervals. Video footages of the fan formation process of the debris flow were acquired using an additional DSLR set at 60 fps (K-3 ii, Ricoh Co.).

The average velocity of the surge front, from the end of the flume to the stoppage in the deposition area, was measured via the video footage. Assuming that the end of the channel is 0 m, the runout distance of the surge front was read from the video footage. The amount of time required to reach this distance was used to measure the travel time. The average velocity was calculated by dividing the distance by the travel time.

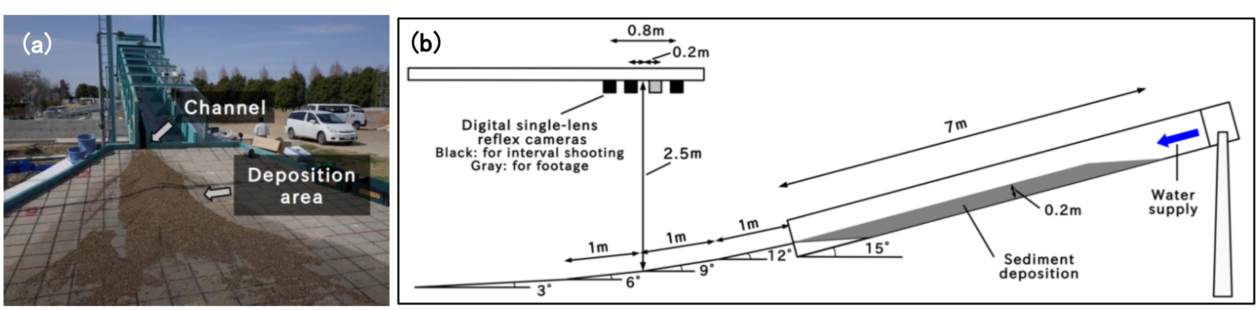


Fig. 1. Experimental setup. (a) View of the channel. (b) Setting of channel and equipment.

We created high-definition digital surface models (DSM) of the debris-flow fan using SfM-MVS software (PhotoScan Professional, Agisoft LLC) from three synchronized photographs. The resolution of the DSMs was set at 1.5 mm, based on the average density of the point cloud. Georeferences were performed using local geographic coordinates of outcropped intersection points of grid lines in the deposition area. In order to test and validate the accuracy of the DSMs, we directly measured the depth of the fan at each intersection point of the deposition area to compare with the DSMs at the end of the experiment.

PIV was used to detect the main flow direction during the fan formation process. We estimated the vectors of surface velocity by the cross-correlation analysis using pairs of photographs (with 1/60-s intervals) extracted from the video footages.

## 3. Results

The first surge produced symmetrical deposition ranges similarly among cases (Fig. 2). The runout of the first surge continued for approximately 30 seconds. The deposition depth of the fan at that time was almost similar to the single surge system (Fig. 3). In contrast, the second surge produced fans that were asymmetrical and had different topography among cases (Figs. 4 and 5), due to the differences in inundation and deposition processes.

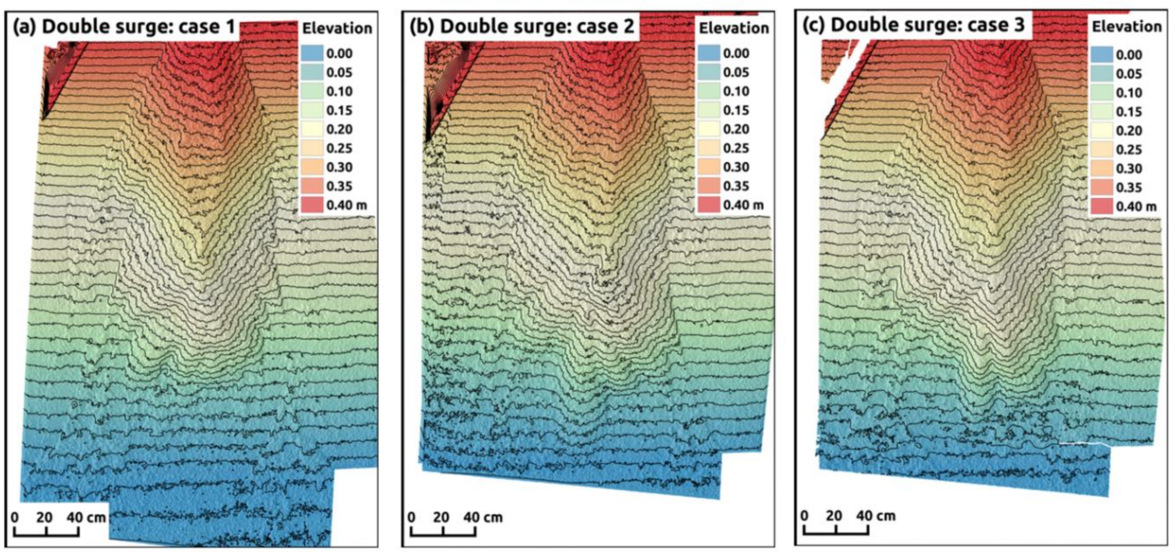


Fig. 2. DSMs of double surge cases after deposition of first surge. (a) case 1. (b) case 2. (c) case 3. Color of the legend indicates elevation when the elevation of the area with a slope of 6° is 0 (3 m from the end of upper channel). The contour interval is 1 cm.

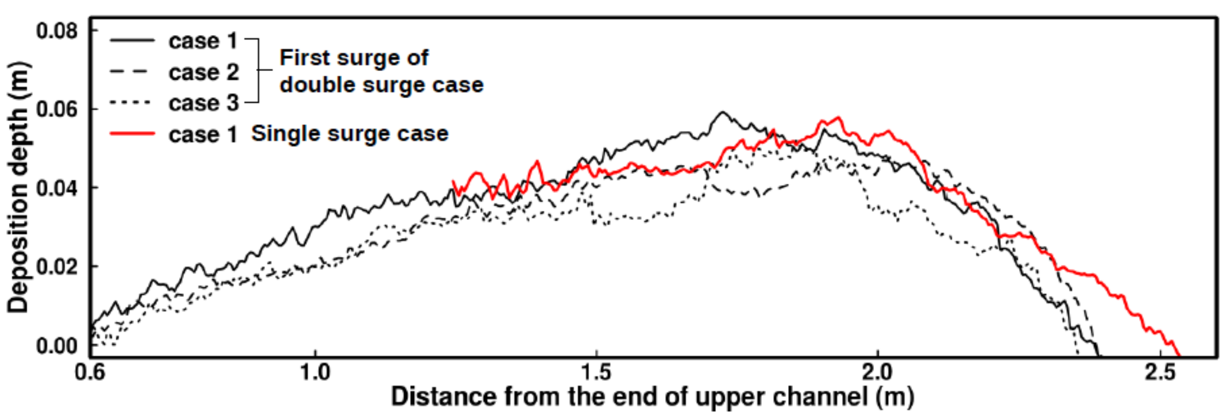


Fig. 3. Comparison of the deposition depths at the center of the fans.The black lines indicate the deposition depths of the fans produced by the first surge. The solid red line indicates the deposition depth of the single surge case after 30 seconds from the start of the run out.

Although the fans tended to bank to the right side in all single surge cases (Fig. 6), the deposition distances reached further downstream and had a greater area compared with those of the double surge cases (Figs. 2-5). Along the edge of the flow path, topography similar to a natural levee was produced, and the bed slope of the path was consistent at approximately 6 degrees.

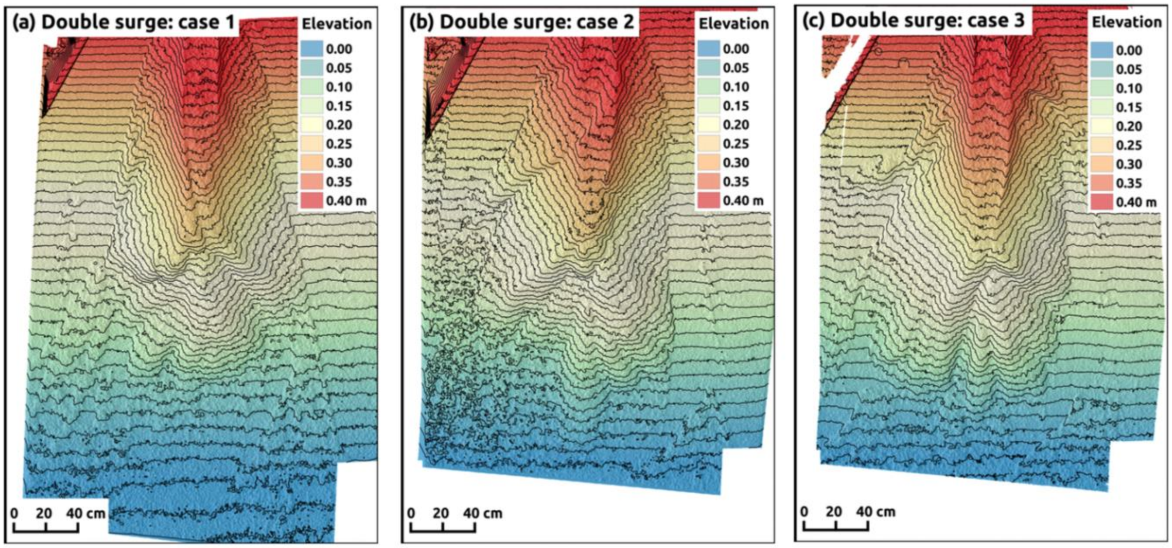


Fig. 4. DSMs of double surge cases after deposition of second surge. (a) case 1. (b) case 2. (c) case 3.

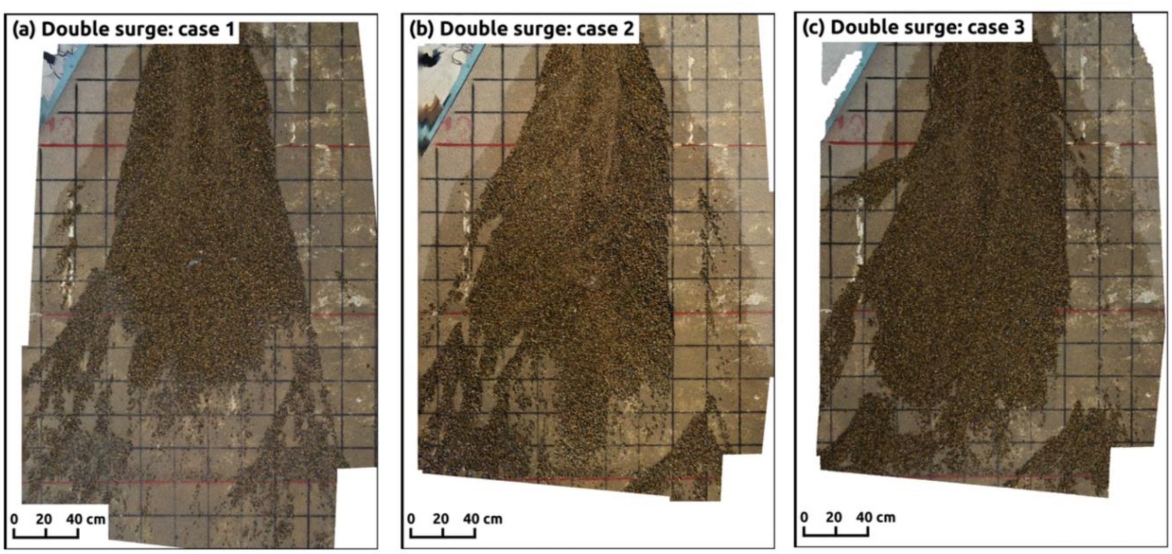


Fig. 5. Photographs of double surge cases after deposition of second surge. (a) case 1. (b) case 2. (c) case 3.

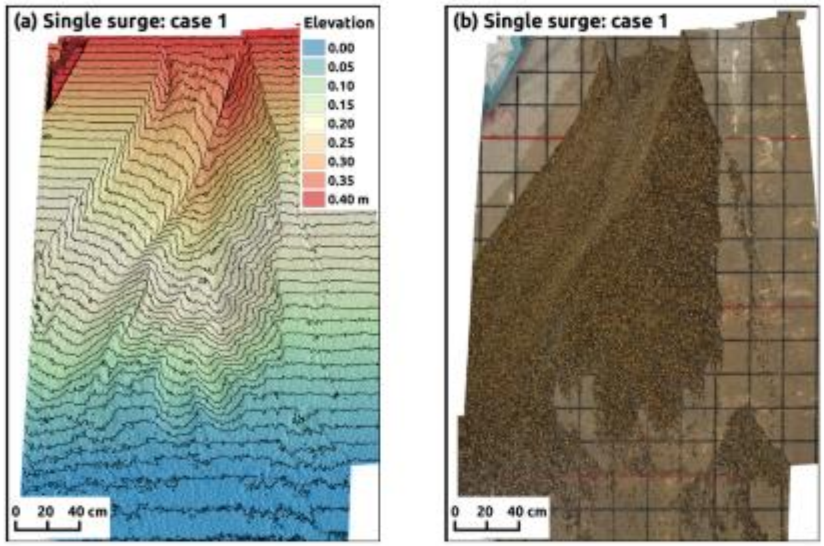


Fig. 6. SfM-MVS results of single surge cases after finish of surge deposition. (a) DSM. (b) Ortho photograph.

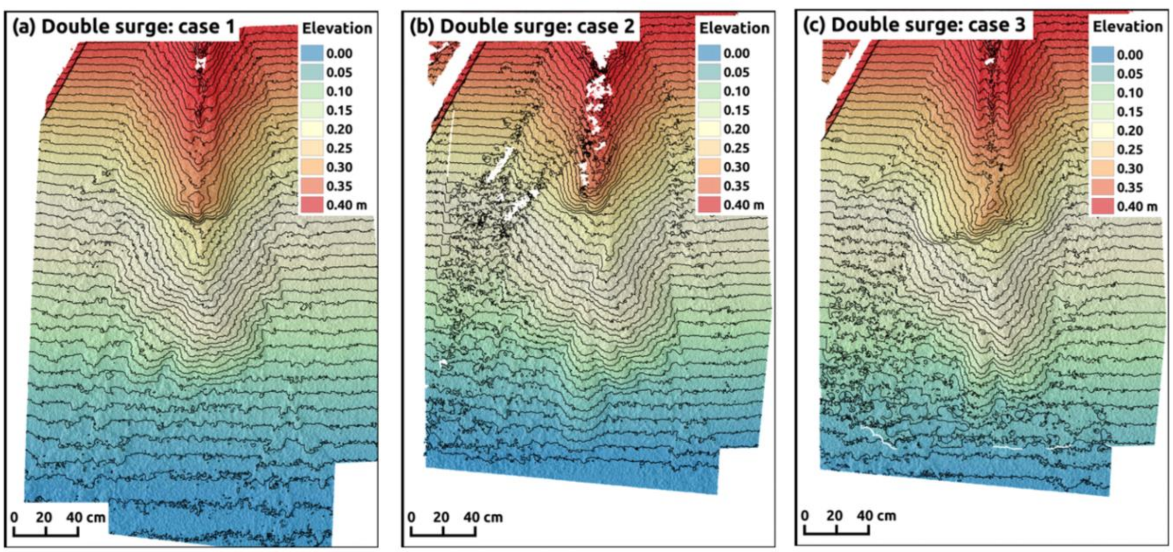


Fig. 7. DSMs of double surge cases after 10 seconds from the start of runout of second surge. (a) case 1. (b) case 2. (c) case 3.

For the double surge cases, the time-series changes in flow path direction of the second surge were different among the cases. The results of SfM-MVS showed that in all cases, the front of the second surge stopped approximately 1.2 m downstream from the outlet of the channel, and above the fan produced by the first surge (Fig. 7). After this stoppage, the flow following the front changed their direction of descent. Fourteen seconds after the start of the runout of the second surge, the flow descended with a right side in cases 1 and 2 (Figs. 8a, b), whereas the flow descended with a left bank in case 3 (Fig. 8c).

The avulsion processes in the flow paths continued and progressed with differentiation in topography. After 4 seconds, the flow directions were changed again in cases 1 and 3 (Figs. 9a, c), whereas the flow continued to descend to the right side in case 2 (Fig. 9b). Consequently, the final topography of the fan inclined to the left bank in case 1 (Fig. 4a), and the right bank in cases 2 and 3 (Figs. 4b, c).

The difference in runout distance of the first surge front between the single and double surge cases was up to 0.2 m (Fig. 10a). However, the difference between the first and second surge for the double surge cases was more significant, with the first surge and the second surge at around 2.8 m and 1.2 m, respectively. Through this decrease in the runout distance, almost all sediment from the second surge deposited upstream at a point where the bed slope changed 6 to 3 degrees. The travel time of the first surge was approximately 6 seconds, whereas the travel time of the second surge was 2 seconds longer at 8 seconds (Fig. 10b). Correspondingly, the velocity of the first surge front was approximately 0.4 m/s, and the velocity of the second surge was 0.18 m/s, less than half of that of the first surge (Fig. 10c).

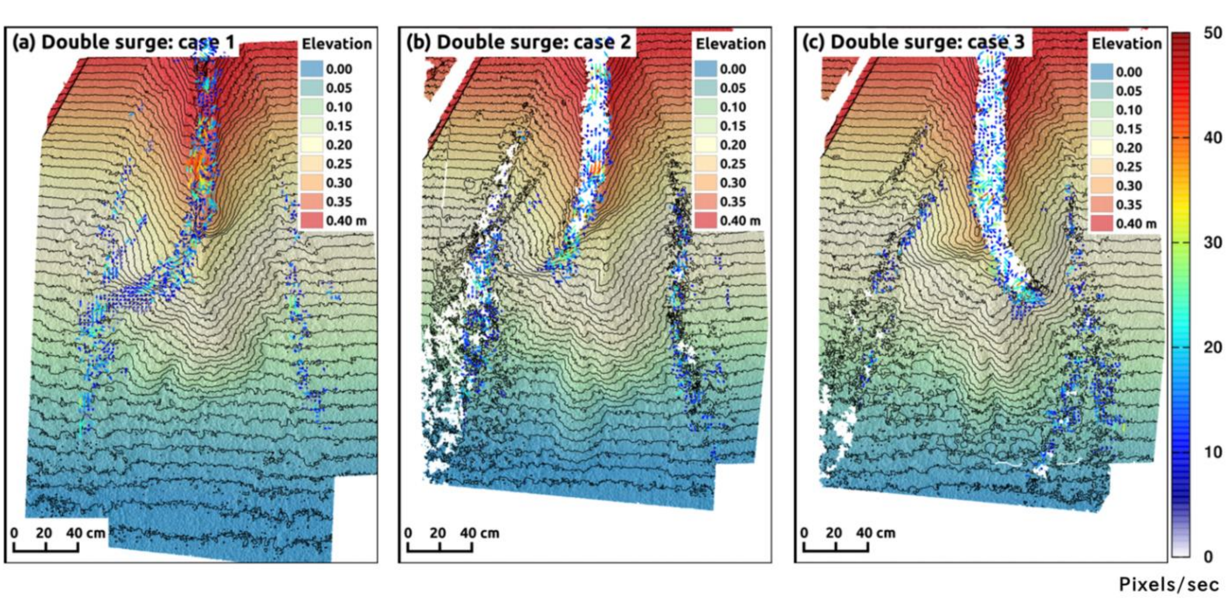


Fig. 8. DSMs of double surge cases after 14 seconds from the start of runout of second surge. (a) case 1. (b) case 2. (c) case 3. Arrows indicate estimated vectors for velocity of debris-flow surface.

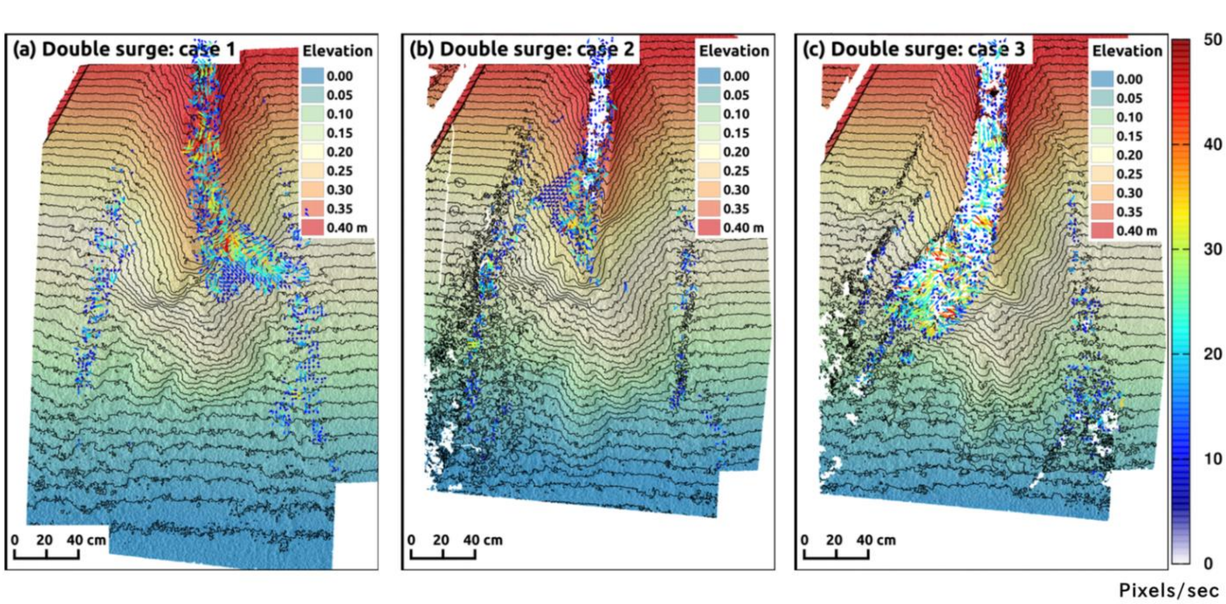


Fig. 9. DSMs of double surge cases after 18 seconds from the start of runout of second surge. (a) case 1. (b) case 2. (c) case 3.

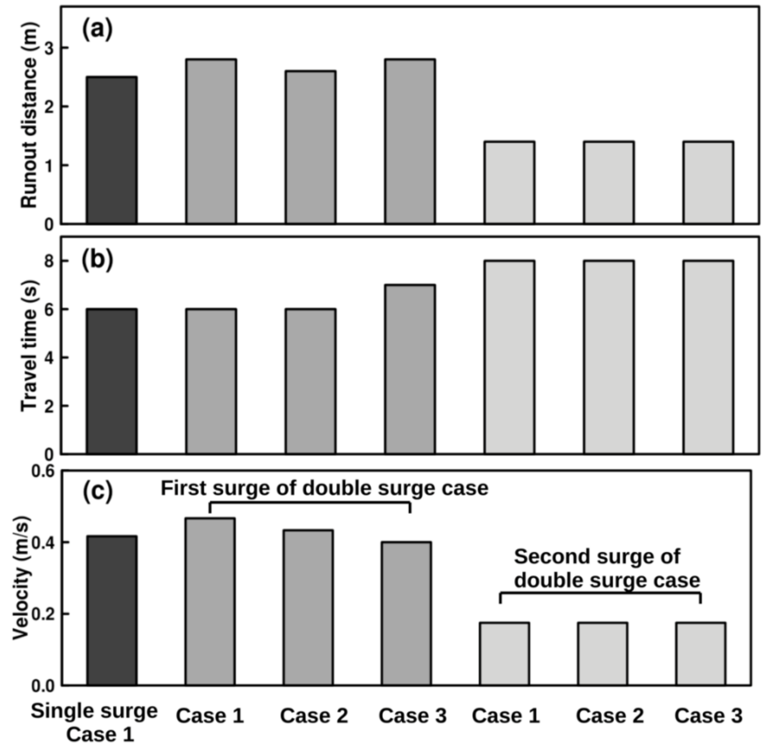


Fig. 10. Characteristics of surge front. (a) Runout distance from the end of upper channel. (b) Travel time from start of run out to stop of front. (c) Average velocity.

## 4. Discussion

The travel distance of the second surge decreased in the double surge system. A larger amount of sediment tended to deposit in the upper and middle portion of the fan when compared to the fan produced by the single surge system. There is a clear indication of backfilling of the channel after the deposition of materials from the initial surge.

In debris-flow mechanics, sediment deposition has been described by the deposition (entrainment) rate equations (Takahashi, 2007). Several deposition rate equations have been proposed (e.g., Takahashi and Kuang, 1986; Egashira et al., 2001; Suzuki et al., 2011). Although the parameters involved in evaluating deposition rate are different among these equations, these equations were based on the concept that the current flow state is transitional to the equilibrium state. Here, the equilibrium state is the state where both deposition and entrainment do not occur due to the steady flow condition (Takahashi, 2007). The flow direction of the single surge cases was fixed due to the development of the channel, with a relatively consistent bed slope surrounded by topographies similar to natural levees. Running through this channel, sediments reached and deposited further downstream compared to the double surge cases. These results indicate that the continuing flow was able to reach further downstream due to the prevention of deposition by the equilibrium bed slope formed by the continuous flow in the fixed channel.

In contrast, the travel distance of the second surge was short, where sediment was deposited upstream with a thick depth. This result implies that the deposition and stoppage of the second surge were induced by the factor differed from the transition from the current flow state to the equilibrium state in the single surge cases. De Haas et al. (2016, 2018) indicated that the low-gradient zones produced by the deposition of previous surges progress the backfilling of channels. Although the runout of the first surge continued for approximately 30 seconds, the deposition depth of the fan at that time was almost similar for all cases. Therefore, the difference in the slope of the fan was small between the single surge and double surge systems until 30 seconds after the start of the runout. This result implies that the deposition of the second surge was affected by not only the slope of the fan but also the condition produced by the intermittency of the surges.

In the double surge cases, there was no surface flow on the fan produced by the first surge when the second surge that was generated by second water supply reached the deposition area. In other words, the surface was in a state that was almost unsaturated. On the unsaturated bed, the deposition of flow is accelerated through the increase in the sheer resistance stress due to the decrease in the pore-fluid pressure at the boundary between the bottom of the flow and the bed surface (Gonda, 2009). Similar deposition patterns induced by unsaturated deposits had been reported before in a field survey (Staley et al., 2011). Therefore, the deposition of the second surge may be caused by the unsaturated fan. The decrease in flow velocity at the front of the second surge also supports the notion that the flow stoppage and deposition was due to the increased resistance on this unsaturated bed.

Importantly, the flow direction shifted through the topographic changes in the fan due to the stoppage of the second surge front. Therefore, the final deposition range of the fan differed among the double surge cases. This result implies that the deposition range may be different among debris-flow where there had been multiple intermittent surges flowing down, even where the hydrograph is similar. This indicates there is a possibility that accurate numerical simulation of the deposition range cannot be achieved even where the correct observed debris-flow hydrograph is being used. Therefore, the representation of the saturation condition in deposition layers needs consideration in order to simulate the fan development process accurately.

## 5. Conclusion

This study demonstrated that double surge cases produce different fan morphology among cases, due to the differences in inundation and deposition range of the second surge. This implies that the unsaturated surface condition of the fan produced by the first surge led to a change in the deposition range of the second surge. These results indicate that a change in the saturated condition of the bed surface induces differentiation in fan morphology. Therefore, examination of characteristics of the fan and surge affecting saturation, such as surge duration and grain-size distribution, is necessary for understanding flow deposition. Additionally, the elucidation of the mechanism of entrainment and deposition of debris flow in relation to the degree of saturation in the bed would be the key to the development of more accurate numerical simulations of debris flow.

## Acknowledgements

The research is supported by JSPS KAKENHI Grant Number 18J01961.

## References

Chen, H.X., Zhang, L.M., Gao, L., Yuan, Q., Lu, T., and Xiang, B., 2017, Simulation of interactions among multiple debris flows: Landslides, v. 14, no. 2, p. 595–615.

De Haas, T., Van Den Berg, W., Braat, L., and Kleinhans, M.G., 2016, Autogenic avulsion, channelization and backfilling dynamics of debris flow fan: Sedimentology, v. 63, no. 6, p. 1596–1619.

De Haas, T., Densmore, A.L., Stoffel, M., Suwa, H., Imaizumi, F., Ballesteros-Cánovas, J.A., and Wasklewicz, T., 2018, Avulsions and the spatio-temporal evolution of debris-flow fans: Earth-Sciences Reviews, v. 177, p. 53–75.

Dowling, C.A., and Santi, P.M., 2014, Debris flow and their toll on human life: a global analysis of debris-flow fatalities from 1950 to 2011: Natural Hazards, v. 71, p. 203–227.

Egashira, S., Honda, N., and Itoh, T., 2001, Experimental study on the entrainment of bed material into debris flow: Physics and Chemistry of the Earth, Part C: Hydrology, Ocean and Atmosphere, v. 26, p. 645–650.

Gonda, Y., 2009, Function of a debris-flow brake: International Journal of Erosion Control Engineering, v. 2, no. 1, p. 15–21.

Nakagawa, H., and Takahashi, T., 1997, Estimation of a debris flow hydrograph and hazard area: *in* Proceedings of 1st International Conference, Debris Flow Hazards Mitigation/Mechanics, Prediction, and Assessment, p. 64–73.

Pederson, C.A., Santi, P.M., and Pyles, D.R., 2015, Relating the compensational stacking of debris-flow fans to characteristics of their underlying stratigraphy: Geomorphology, v. 248, p. 47–56.

Staley, D.M., Wasklewicz, T.A., Coe, J.A., Kean, J.W., McCoy, S.W., and Tucker, G.E., 2011, Observations of debris flows at Chalk Cliffs, Colorado, USA: Part 2, changes in surface morphometry from terrestrial laser scanning in the summer of 2009: *in* Proceedings of 5th International Conference. Debris Flow Hazards Mitigation/Mechanics, Prediction, and Assessment, p. 759–768.

Suzuki, T., Hasegawa, Y., Mizuno, H., and Osanai, N., 2011, Numerical simulation method of debris flow introducing the non-entrainment erosion rate equation, at the transition point of the riverbed gradient or the channel width and in the area of sabo dam: *in* Proceedings of 5th International Conference. Debris Flow Hazards Mitigation/Mechanics, Prediction, and Assessment, p. 615–622.

Takahashi, T., and Kuang, S.F., 1986, Formation of debris flow on varied slope bed: Annals of the Disaster Prevention Research Institute, Kyoto University, v. 29, no. B-2, p. 345–359. (In Japanese with English summary)

Takahashi, T., 2007, Debris Flow: Mechanics, Prediction and Countermeasures: Taylor and Francis, Balkema. pp 448.